

B. PSZCZÓŁKOWSKI<sup>1\*</sup>, M. BRAMOWICZ<sup>1</sup>, W. REJMER<sup>1</sup>,  
T. CHROSTEK<sup>1</sup>, C. SENDEROWSKI<sup>1</sup>

## THE INFLUENCE OF THE PROCESSING TEMPERATURE OF POLYLACTIDE ON GEOMETRIC STRUCTURE OF THE SURFACE USING FDM TECHNIQUE

The influence of the processing temperature of polylactide (PLA) on the structure geometry changing (SGC) and its functional properties were analyzed. The PLA samples subjected to testing were manufactured using incremental fused deposition modeling technology (FDM) with processing temperatures ranging from 180°C to 230°C. The topography of the PLA surfaces formed during heat dissipation and generated by the work table was analyzed. The roughness measurements were carried out using the profile method in accordance with PN ISO 3274: 2011. Registered profiles of the surfaces were analyzed numerically in fractal terms using the method of the  $S(\Delta x)$  structure function. The functional properties of the PLA surface were evaluated on the basis of Abbott-Firestone curves, according to PN EN ISO 13565-2: 1999.

*Keywords:* FDM, polylactide PLA, surface analysis

### 1. Introduction

Modern technological development and the need for rapid prototype production (RPP) have resulted in a rapid increase in demand for special-purpose components, often having a very complex structure. The task of modern manufacturing techniques is to ensure the right quality of products, with short production times and minimal costs. Therefore, when developing production processes, it is necessary to choose such a technology that will affect the properties of the object already during the manufacturing process [1]. Additive production methods that enable three-dimensional faithful reproduction of objects are a promising solution, and by modulating the processing of the input material also affect its mechanical, functional and chemical properties [2,3].

Additive manufacturing technology requires appropriate materials which processing will be simple and low cost. The solution turned out to be thermoplastic materials, however, they must meet a number of standards related to safety and harmless processing. Therefore, the polylactide (PLA) called also polyactic acid could be the good solution to many applications. It is a thermoplastic polymer belonging to the group of aliphatic polyesters, produced from natural renewable raw materials, such as: corn meal, sugar beets and sugar cane [4,5]. It is character-

ized by complete biodegradability, good mechanical properties in relation to low density and high biocompatibility with a living organism [2,6].

These properties are a cause of interest in the medical community, especially after the FDA (Food and Drug Administration) recognized it in 1970 as safe for living organisms [7,8]. Every interference in a living organism through the introduction of a foreign body is associated with the reaction of the immune system, which is why it is sought to replace durable metal implants with polymeric materials capable of degradation after a specified time and fulfilling of their function [9-11]. Therefore, in recent years there has been a significant intensification of research on the properties of PLA in terms of application in medicine [12,13].

Poly lactide in connection with FDM technologies is used, among others in the design and production of cellular scaffolds (suits). To this aim, some methods are being developed for producing a substrate environment for rebuilding living native tissue on special cellular scaffolds implanted into organisms [14]. The cells are deposited on elements with a porous structure that allows tissue to grow deep into the scaffolding and the formation of blood vessels.

One of the RPP methods of suits creation are Fused Deposition Modeling (FDM) technologies, which the head temperature

<sup>1</sup> UNIVERSITY OF WARMIA AND MAZURY IN OLSZTYN, FACULTY OF TECHNICAL SCIENCES, 11 OCZAPOWSKIEGO STR., 10-719 OLSZTYN, POLAND

\* Corresponding author: bartosz.pszczolkowski@uwm.edu.pl



plays a significant impact on the geometry of paths applied during the production of elements [15,16]. This one affects the topography of individual paths, which in consequence will have a significant impact on the development of biological material on the surface of the produced element [16]. In addition, PLA is used in modern pharmacy in the production of intelligent drugs, in which the release of the active substance occurs along with the progressive degradation. It creates the opportunity to develop the so-called “Smart medicine”, which will be tasked to apply the right amount of active substance to a specific place in the body, sometimes in the place disease processes origin so called “Targeted therapy” [17]. Research on this type of modern forms of medicine has been intensively conducted for almost sixty years [18].

Its ability to break down automatically and compostability caused that it also quickly became an attractive substitute for the currently used polyethylene, polypropylene or polystyrene [13].

The high demands placed on both biodegradable implants and everyday objects force the development of modern methods for accurate characterization and description of the geometrical structure of the implants surface. In addition to chemical biocompatibility, surface properties enabling the development of biological material and keeping the medium ensuring their gradual degradation are important [19]. The most important of them are: porosity, roughness, degree of surface development and directionality [14,20].

Results of research conducted by E. Mazgajczyk and others [16] indicate that the increase in PLA processing temperature in the range of 190-210°C using FDM technology, affects the height and width of the paths structure. As temperature increases, the paths become lower, while their width tends to be inversely proportional to the growth [16,21]. Therefore, it is important to know the effect of temperature on the geometric structure and functional properties of PLA surfaces.

## 2. Experimental

The modeled disk-shaped elements with a diameter of 40 mm and a thickness of 1 mm were made of PLA using FDM technology with a 1.75 mm diameter filament.

Constant printing parameters were: nozzle diameter 0.4 mm, platform temperature 50°C, layer pitch 0.2 mm, printing speed 1800 mm/min. The variable process parameter was the extruder temperature. The FDM processing of PLA material was carried out in the temperature range from 180°C to 230°C, in increments of 10°C, obtaining 6 states of samples given to the surface analysis tests. For every state 4 samples were obtained for investigative purposes.

The geometrical structure and functional properties of the surface were analyzed in accordance with PN-ISO 3274 on the basis of 2D profiles measurements carried out using the Mitutoyo SurfTest SJ-210 profilometer with a measuring needle with a 60° angle of inclination and a rounding radius of 2 μm. The measuring length ( $L$ ) consisted of five elementary sections with a length  $L_c = 0.8$  mm. The change of amplitude ( $Ra$ ,  $Rq$ ,  $Rz$ ) and functional parameters ( $R_{pk}$ ,  $R_k$ ,  $R_{vk}$ ) of the surface were analyzed in accordance with PN-EN ISO 4287: 1997 and PN-EN ISO 13565-2: 1999.

Similarity assessment and the degree of surface development were carried out using the structure function  $S(\Delta x)$ .

## 3. Fractal analysis using the structure function method

The structure function  $S(\Delta x)$  described by the equation (1) is presented the vertical relationships between two points of the surface profile distant from each other by the vector  $\Delta x$  [22]. An example of the course of the function  $S(\Delta x)$  and the corresponding surface topography profile are shown in Fig. 1. Analysis of the waveform structure function  $S(\Delta x)$  course allows the determination of the fractal dimension ( $D$ ) and the corner

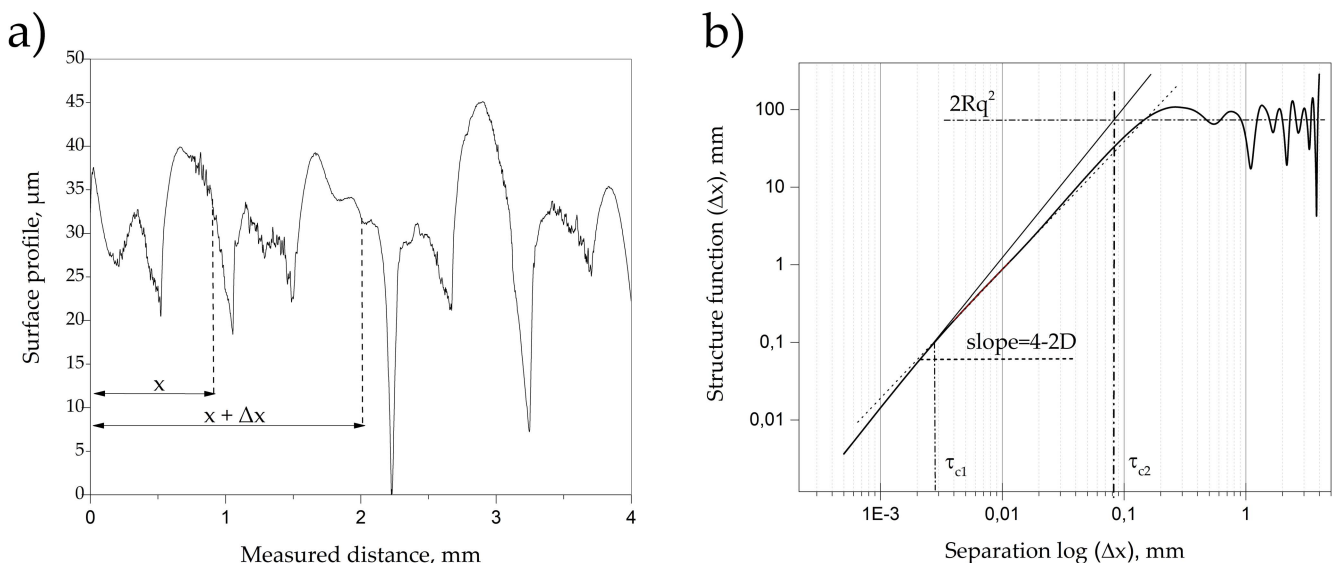


Fig. 1. (a) Surface topography profile and (b) the corresponding course of the waveform structure function  $S(\Delta x)$

frequency  $\tau_c$  (threshold length) in which the surface profile shows fractal properties [22]. In the case of a profile, the value of the fractal dimension is within  $1 < D < 2$ , with 1 corresponding to a straight line, and 2 to an extremely developed line, i.e. consisting of infinitely many components.

$$S(\Delta x) = \left\langle |h(x) - h(x + \Delta x)|^2 \right\rangle \quad (1)$$

where:

- $h(x)$  – profile height at the  $x$  coordinate point,
- $\Delta x$  – distance between two points of the profile,
- $\langle \rangle$  – is the average value.

According to what was shown in [23] on the basis of fractal geometry for solid surfaces, the structure function takes the form of equation (2):

$$S(\Delta x) = CL^{2(D-1)}\Delta x^{(4-2D)} \quad (2)$$

where:

- $C$  – constant value,
- $L^{2(D-1)}$  – surface profile topthesis,
- $D$  – fractal dimension.

An example of the topography profile of the surfaces studied and the corresponding structure function are shown in Fig. 1.

As can be seen in Fig. 1b, the function  $S(\Delta x)$  after exceeding the threshold length value ( $\tau_c$ ) seeks to establish its value, which is equal to  $2R_q^2$ . It also sets a border separating the short-wave signal from the long-wave signal [24].

#### 4. Functional properties of the surface

The functional properties of the surface were assessed based on load-bearing curves, called also Abbott-Firestone (A-F) curves [25]. They show the percentage of material at different heights of the surface profile (Fig. 2). The A-F function was used to indicate the characteristic parameters, as:  $R_{pk}$  – reduced height of peaks without bearing properties,  $R_k$  – height of the roughness core, characterizing the surface bearing properties,  $R_{vk}$  – reduced depth of valleys, characterizing the ability of the surface to hold liquids,  $S_{mr1}$ ,  $S_{mr2}$  – percentage of the lower and upper fractions.

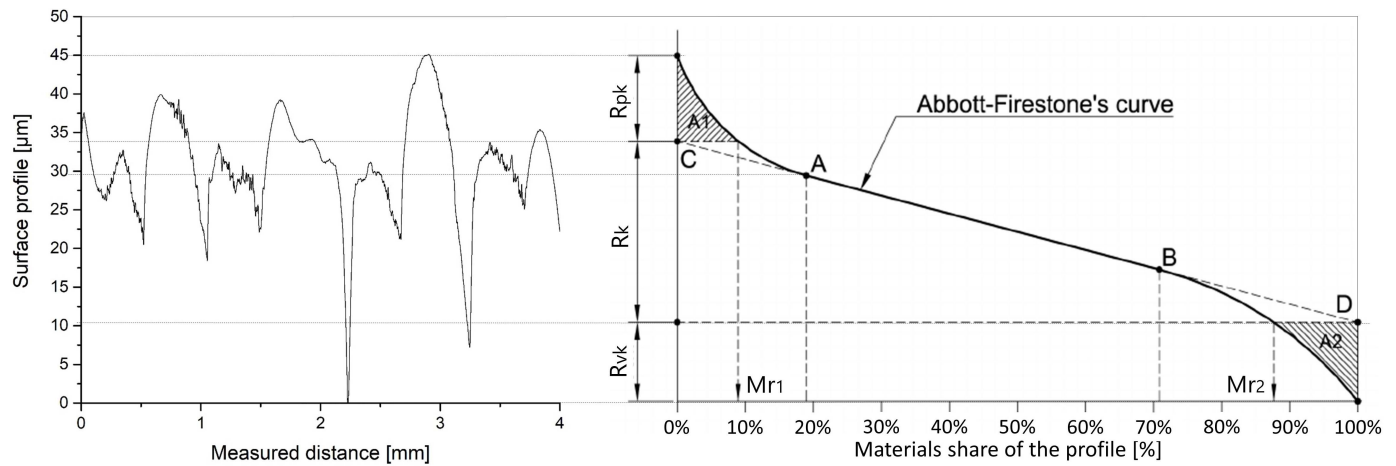


Fig. 2. Topography profile of the surface and the corresponding Abbott-Firestone curve

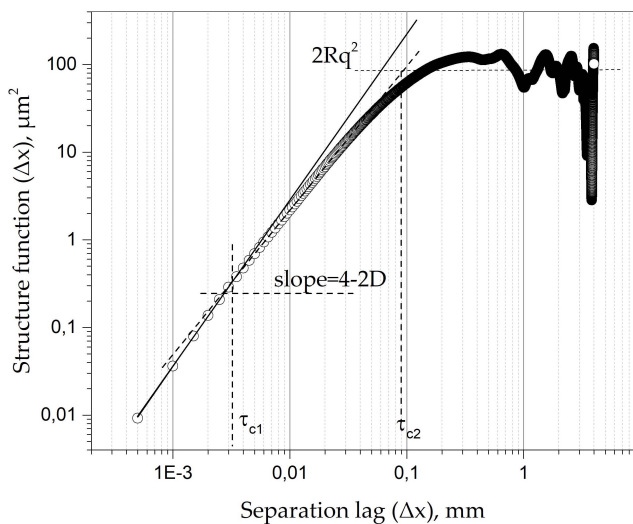


Fig. 3. Example of the function of layered bifractic structure printed in FDM technology

#### 5. Results and discussion

The analysis of the geometric structure for the examined surfaces suggests a bifractal structure of layers constituted by the FDM method. In the case of bifractal structures, such as agglomerates, the first fractal dimension characterizes the constituent element of the agglomerate, while the second describes their arrangement on the surface [26,27]. In the analyzed cases, the generated structure functions have characteristic inflection points corresponding to the threshold length  $\tau_{c1}$  determining the cluster length and  $\tau_{c2}$  determining the range of self-similarity. Fig. 3 shows an example of the  $S(\Delta x)$  waveform structure function obtained for surfaces constituted by FDM technology.

Obtained results of the fractal analysis (Table 1) indicate that the first fractal dimension  $D1$  does not show too much temperature dependence. Its value varies from 1.05 to 1.02, which is only a change of 3%, but the downward trend is maintained

with increasing PLA processing temperature. Therefore, it can be assumed that the area of forming clusters is decreasing.

Another character of the changes is shown by the D2 parameter, which value clearly decreases from the maximum value of 1.23 at 190°C to a constant value at temperature higher than 210°C (Fig. 4). The similar nature of the changes is assumed by the threshold length  $\tau_{c2}$  (Fig. 5), which indicates that the surface development gradually decreases with temperature. This should be associated with the increase in track width of PLA shown in [17].

The results of the tests also indicate that the increase in processing temperature using FDM technology causes noticeable changes in the roughness parameters  $R_a$  and  $R_q$  (Fig. 6 and Fig. 7). An increase in the average and mean square surface

profile deviation from the average lines produced, especially for temperature above 190°C, is observed. A similar trend is adopted by the total height of the  $R_t$  profile falls in the range of 180–200°C and then increases linearly by a constant value in the range of 210–230°C. The functional parameters of the surface are also changing. The depth of the valleys decreases by about 35% from the maximum value at 190°C to 20.083  $\mu\text{m}$  at 230°C (Fig. 10). This indicates a decreased ability of the surface to hold liquids. A similar trend of changes is shown in the reduced height of sharp elevations, which, although they do not have supporting properties, but can be the attachment points for biological material to develop on the surface of the suits. Detailed results of the roughness measurements and functional parameters are summarized in Table 2. As already mentioned, the lowest ability

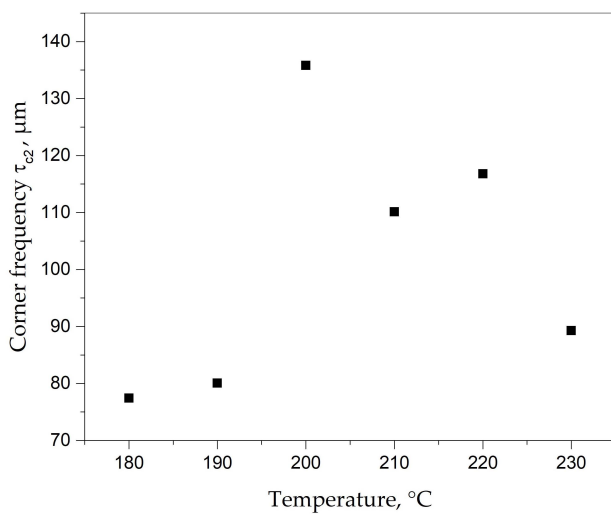


Fig. 4. Dependence of the threshold length  $\tau_{c2}$  on the processing temperature

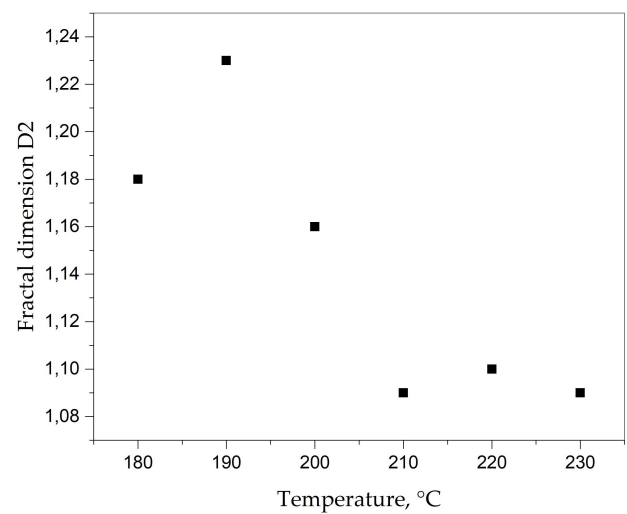


Fig. 5. Dependence of the fractal dimension  $D2$  on the processing temperature

TABLE 1

The degree of change in surface structure development with increasing temperature:  $D$  – fractal dimension and  $\tau_c$  – corner frequency

Process Temperature [°C]	D1	D2	$\tau_{c1}$ [ $\mu\text{m}$ ]	$\tau_{c2}$ [ $\mu\text{m}$ ]
180	1.05 $\pm$ 0.018	1.18 $\pm$ 0.058	3.795 $\pm$ 0.061	77.426 $\pm$ 3.94
190	1.05 $\pm$ 0.005	1.23 $\pm$ 0.034	4.059 $\pm$ 0.209	80.068 $\pm$ 12.49
200	1.05 $\pm$ 0.008	1.16 $\pm$ 0.026	3.746 $\pm$ 0.045	135.82 $\pm$ 7.58
210	1.03 $\pm$ 0.050	1.09 $\pm$ 0.010	4.377 $\pm$ 0.346	110.13 $\pm$ 5.59
220	1.03 $\pm$ 0.006	1.10 $\pm$ 0.023	4.197 $\pm$ 0.123	116.79 $\pm$ 11.39
230	1.02 $\pm$ 0.009	1.09 $\pm$ 0.021	4.84 $\pm$ 0.111	89.293 $\pm$ 26.26

TABLE 2

Summary of surface parameters

Temp. [°C]	$R_q$ [ $\mu\text{m}$ ]	$R_a$ [ $\mu\text{m}$ ]	$R_t$ [ $\mu\text{m}$ ]	$R_k$ [ $\mu\text{m}$ ]	$R_{vk}$ [ $\mu\text{m}$ ]	$R_{pk}$ [ $\mu\text{m}$ ]	$S_{mr1}$ [%]	$S_{mr2}$ [%]
180	5.68 $\pm$ 0.57	4.46 $\pm$ 0.48	45.12 $\pm$ 14.61	12.65 $\pm$ 2.21	47.31 $\pm$ 12.11	7.73 $\pm$ 1.29	16.17 $\pm$ 4.52	87.11 $\pm$ 3.38
190	5.65 $\pm$ 0.48	4.48 $\pm$ 0.38	28.91 $\pm$ 2.28	13.35 $\pm$ 1.75	58.08 $\pm$ 1.36	2.35 $\pm$ 2.71	4.60 $\pm$ 1.25	77.90 $\pm$ 0.49
200	5.87 $\pm$ 0.51	5.01 $\pm$ 0.42	24.78 $\pm$ 1.60	16.98 $\pm$ 1.56	30.91 $\pm$ 1.63	4.37 $\pm$ 1.07	10.10 $\pm$ 1.37	89.15 $\pm$ 2.82
210	6.42 $\pm$ 0.18	5.53 $\pm$ 0.25	33.01 $\pm$ 2.16	18.93 $\pm$ 2.47	32.29 $\pm$ 3.44	6.46 $\pm$ 1.86	12.15 $\pm$ 1.68	86.77 $\pm$ 2.59
220	6.89 $\pm$ 0.35	5.84 $\pm$ 0.31	36.03 $\pm$ 3.54	18.43 $\pm$ 1.20	21.96 $\pm$ 4.29	10.07 $\pm$ 2.75	14.53 $\pm$ 5.07	92.63 $\pm$ 3.98
230	7.01 $\pm$ 0.32	6.10 $\pm$ 0.26	39.34 $\pm$ 2.62	20.46 $\pm$ 2.62	20.08 $\pm$ 2.29	14.08 $\pm$ 2.95	11.06 $\pm$ 2.60	94.14 $\pm$ 3.55

$R_q$  – root-mean-square deviation of the profile;  $R_a$  – arithmetic mean deviation of the profile;  $R_t$  – total height of the profile;  $R_k$  – depth of the roughness core profile;  $R_{vk}$  – reduced valley depth;  $R_{pk}$  – reduced peak height;  $S_{mr}$  – material share

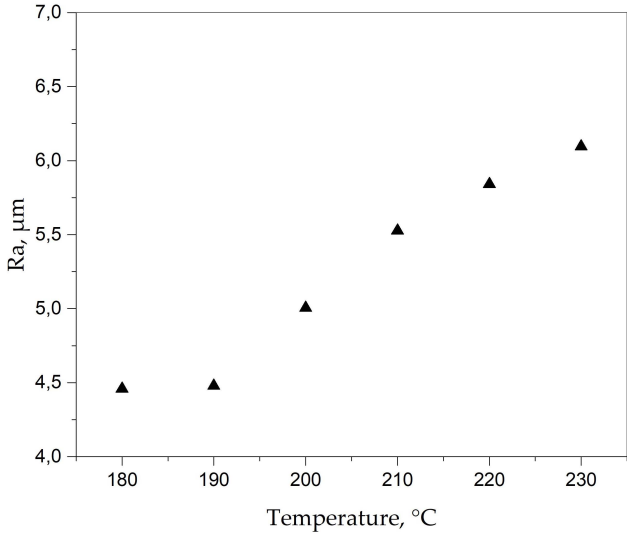


Fig. 6. Dependence of the  $Ra$  parameter on the printing temperature

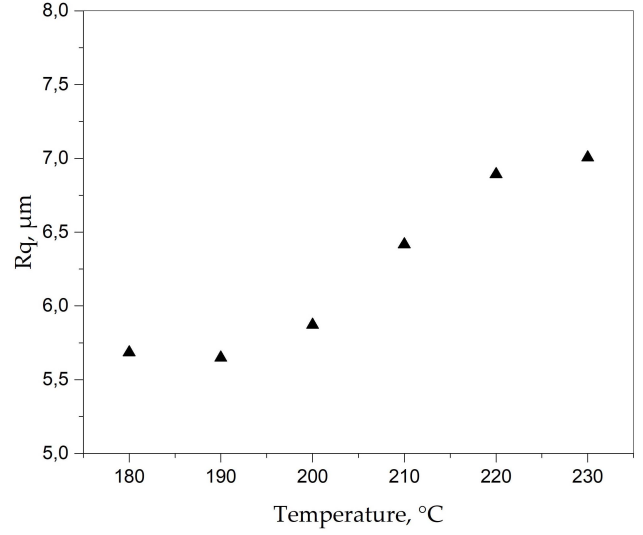


Fig. 7. Dependence of the  $Rq$  parameter on the printing temperature

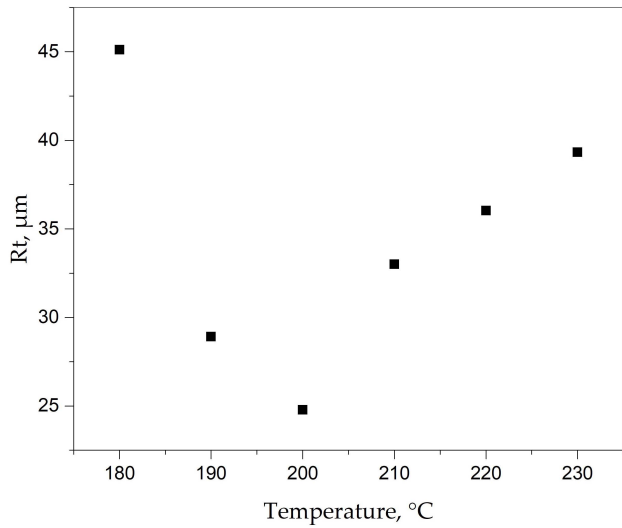


Fig. 8. Dependence of the  $Rt$  parameter on the printing temperature

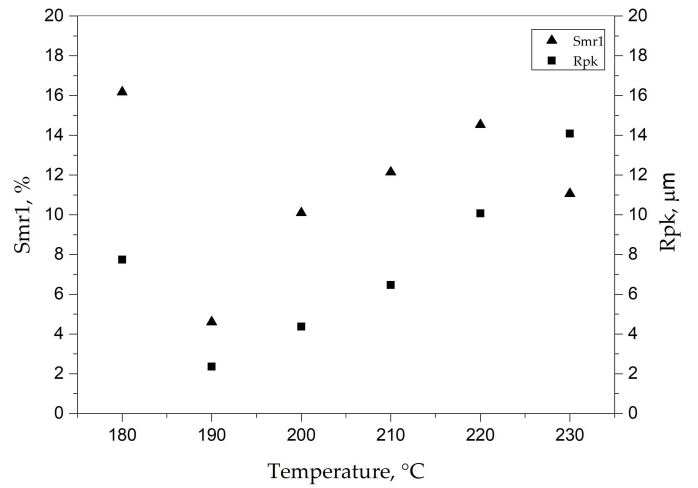


Fig. 9. Relation of the percentage of the upper surface area  $S_{mr1}$  and reduced height of  $R_{pk}$  peaks on the printing temperature

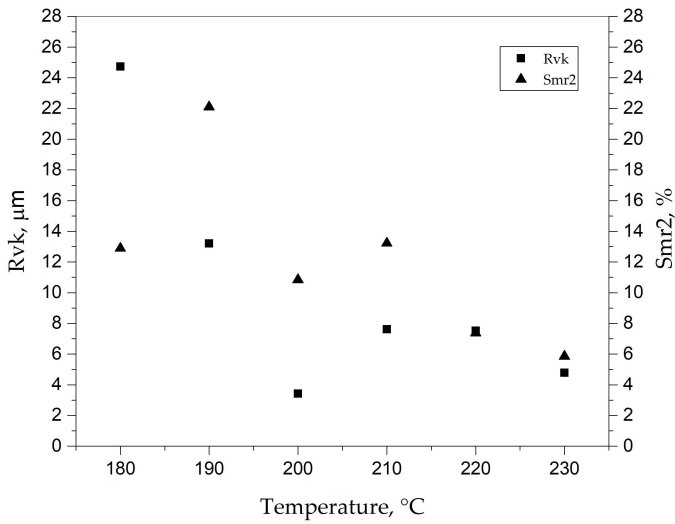


Fig. 10. Relation of the percentage of the upper surface area  $S_{mr2}$  and reduced height of  $R_{vk}$  peaks on the printing temperature

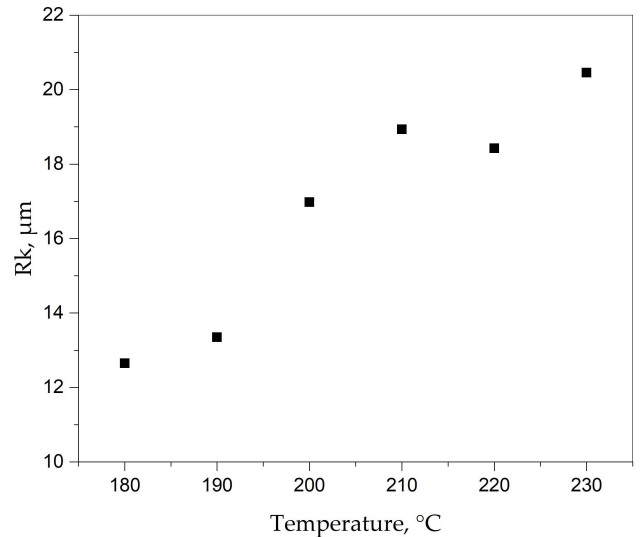


Fig. 11. Dependence of the  $R_k$  parameter on the printing temperature

to transfer loads is demonstrated by components made at 190°C. The surface formed at this temperature is characterized by a small share of peaks (about 4.6%), with a very high proportion of valleys (22%), while the core height is 12.654  $\mu\text{m}$  (Figs. 9-11). Therefore, the surface has the greatest fluid holding capacity, which may be beneficial in biodegradation processes.

A similar effect on the surface topography of the polylactide material is exerted by the energy supplied to the printing machine, which indirectly translates into the printing temperature, as demonstrated in [28]. The performed fractal analysis confirms the results of the research contained in the work [16], in which it was found that an increase in printing temperature causes flattening of PLA paths and an increase in their width, which translates into the degree of surface development. The higher temperature of the melted filament causes its spreading on the surface, the width of the paths increases, and thus a smaller amount of them on the produced surface.

## 5. Conclusions

Research on the influence of printing temperature on the surface topography obtained elements using FDM technology revealed a cluster geometric structure of the surface. The results of profilometric measurements revealed that the increase temperature in PLA processing causes an increase in the bearing properties of the surface profile. At the same time, it gradually is reduced the percentage share of valleys and depth, which may indicate a decreasing susceptibility material to biodegradation. On the other hand, the number of sharp hills increases, which, in fact, do not have load-bearing properties, but can be convenient points for the incubation of biological material on the surface of printed elements. Therefore, it could be asserted that by modulating the temperature in FDM processes, it can obtain the desired performance properties, e.g. for use on scaffold structures.

## REFERENCES

- [1] T.-C. Yang, *Polymers-Basel* **10** (9), 976 (2018), DOI: 10.3390/polym1009097.
- [2] M. Grasso, L. Azzouz, P. Ruiz-Hincapie, M. Zarrelli, G. Ren, *Rapid Prototyping J.* **24** (8), 1337-1346 (2018), DOI: 10.1108/RPJ-04-2017-0055.
- [3] M.A. Caminero, J.M. Chacón, E. García-Plaza, P.J. Núñez, J.M. Reverte, J.P. Becar, *Polymers-Basel* **11** (5), 799 (2019).
- [4] L. Xiao, B. Wang, G. Yang, M. Gauthier, *Poly(Lactic Acid)-Based Biomaterials: Synthesis, Modification and Applications* (2012), DOI: 10.5772/23927.
- [5] Z. Foltynowicz, P. Jakubiak, *Polimery-w.* **47**, 769-774 (2002).
- [6] A. Kruk, A. Gadomska-Gajadur, P. Ruśkowski A. Chwojnowski, L. Synoradzki, *Polimery-w.* **2**, 118-126 (2017), DOI dx.doi.org/10.14314/polimery.2017.118.
- [7] R.M. Rasal, A.V. Janorkar, D.E. Hirt, *Prog. Polym. Sci.* **35**, 338-356 (2010).
- [8] A. Duda, *Przem. Chem.* **82**, 905-907 (2003).
- [9] A.C. Vieira, J.C. Vieira, R.M. Guedes, A.T Marques, *Mater. Sci. Forum.* **636-637**, 825-832 (2010), DOI: 10.4028/www.scientific.net/MSF.636-637.825.
- [10] A.C. Vieira, J.C. Vieira, R.M. Guedes, A.T. Marques, V. Tita, *Mater. Sci. Forum.* **730-732**, 56-61 (2013), DOI: 10.4028/www.scientific.net/MSF.730-732.56.
- [11] M. Deng, J. Zhou, G. Chen, D. Burkley, Y. Xu, *Biomaterials.* **26**, 4327-4336 (2005), DOI:10.1016/j.biomaterials.2004.09.067.
- [12] L. Xiao, B. Wang, G. Yang, M. Gauthier, *Poly(Lactic Acid)-Based Biomaterials: Synthesis, Modification and Applications in: D.N Ghista (Eds.), Biomedical Science, Engineering and Technology, InTech* (2012), DOI: 10.5772/23927.
- [13] A. Duda, S. Penczek, *Polimery-w.* **48**, 16-27 (2003).
- [14] P. Szymczyk, A. Pawlik, G. Ziółkowski, B. Dybała, E. Chlebus, *Curr. Prob. Biomech.* **7**, 157-162 (2013).
- [15] C.M. Murphy, M.G. Haugh, F.J. O'Brien, *Biomaterials.* **31**, 461-466 (2010).
- [16] E. Mazgajczyk, P. Szymczyk, E. Chlebus, *Aktualne Problemy Biomechaniki* **8**, 109-114 (2014).
- [17] K. Terlega, M. Lachota, *Pol. Merk. Lek.* **33**, 229 (2012).
- [18] P. Ruśkowski, A.A. Gadomska-Gajadur, *Tworzywa Sztuczne w Przemysle* **2**, 32-35 (2017).
- [19] S. Guessasma, S. Belhabib, H Nouri, *Polym. Test.* **77**, 105924 (2019), DOI: 10.1016/j.polymertesting.2019.105924.
- [20] E. García-Plaza, P.J. Núñez, M.A. Caminero, J.M. Chacón, *Polymers-Basel* **11** (10), 1581 (2019).
- [21] V.E. Kuznetsov, A.N. Solonin, A. Tavitov, O. Urzhumtsev, A. Vakulik, *Rapid Prototyping Journal* **26** (1), 107-121 (2020), DOI: 10.1108/RPJ-01-2019-0017.
- [22] B.B. Mandelbrot, *Fractals Form, Chance and Dimension*, W.H. Freeman & Company (1977).
- [23] M.V. Berry, *J. Phys. A-Math. Gen.* **12**, 781-797 (1979).
- [24] R.S. Styles, T.R. Thomas, *Wear.* **42**, 236-276 (1977).
- [25] E. J. Abbott, F.A. Firestone, *J. Mech. Eng.* **55**, 569-572 (1933).
- [26] M. Bramowicz, L. Braic, F. Ak Azem, S. Kulesza, I. Birlik, A. Vladescu, *Appl. Surf. Sci.* **379**, 338-346 (2016). doi.org/10.1016/j.apsusc.2016.04.077
- [27] K.J. Stout, P.J. Sullivan, W.P. Dong, E. Mainsah, N. Luo, *The development of methods for the characterisation of roughness in three dimensions*, Brussels-Luxembourg and Authors, Commission of the European Communities (1993).
- [28] T. Peng, F. Yan, *CIRP.* **69**, 106-111 (2018).